Physics – Uspekhi **51** (8) 839 – 859 (2008)

CONFERENCES AND SYMPOSIA

PACS numbers: 01.10.Fv, 01.30.Cc; 61.46.Bc, 71.45.Gm, **81.07. – b**;
52.27.Ep, 97.10.Ld, 97.60.Jd; 63.20.kp, **63.22. – m**

Plasma phenomena in nanostructures and neutron stars
Scientific session of the Physical Sciences Division of the Russian Academy of Sciences (26 March 2008)

V V Klimov; Ya N Istomin; Yu A Kosevich

DOI: 10.1070/PU2008v051n08ABEH006794

A scientific session of the Physical Sciences Division of the Russian Academy of Sciences (RAS) was held on 26 March 2008 at the conference hall of the P N Lebedev Physical Institute, RAS. The following reports were presented at the session:

(1) **Klimov V V** (P N Lebedev Physical Institute, RAS, Moscow) "Nanoplasmonics";

(2) **Istomin Ya N** (P N Lebedev Physical Institute, RAS, Moscow) "Electron – positron plasma generation in the magnetospheres of neutron stars";

(3) **Kosevich Yu A** (N N Semenov Institute of Chemical Physics, RAS, Moscow) "Multichannel propagation and scattering of phonons and photons in low-dimension nanostructures".

An abridged version of these reports is given below.

PACS numbers: 61.46.Bc, 71.45.Gm, **81.07. – b**
DOI: 10.1070/PU2008v051n08ABEH006595

Nanoplasmonics

V V Klimov

Advances in the production and visualization of nano-sized clusters and other metal nanoparticles (Fig. 1) have given rise to nanoplasmonics, an important and fast-developing area of nanotechnology and nanooptics. Aimed at designing complex optical nanodevices, nanoplasmonics studies phenomena related to oscillations of conduction electrons in metal nanostructures and nanoparticles and how these oscillations interact with light, atoms, and molecules. Plasmon oscillations in nanoparticles differ considerably from surface plasmons [1] and are therefore called localized plasmons.

What is most special about nanoplasmonic phenomena is that the strong spatial localization of the electronic oscillations is combined with their high frequencies varying from UV to IR ranges. The strong localization, in turn, leads to a huge strengthening of local optical and electric fields. Finally, the properties of localized plasmons are critically dependent on the nanoparticle shape, enabling their resonance systems

Uspekhi Fizicheskikh Nauk **178** (8) 875 – 896 (2008)
DOI: 10.3367/UFNr.0178.200808f.0875
Translated by E G Strel'chenko; edited by A Radzig

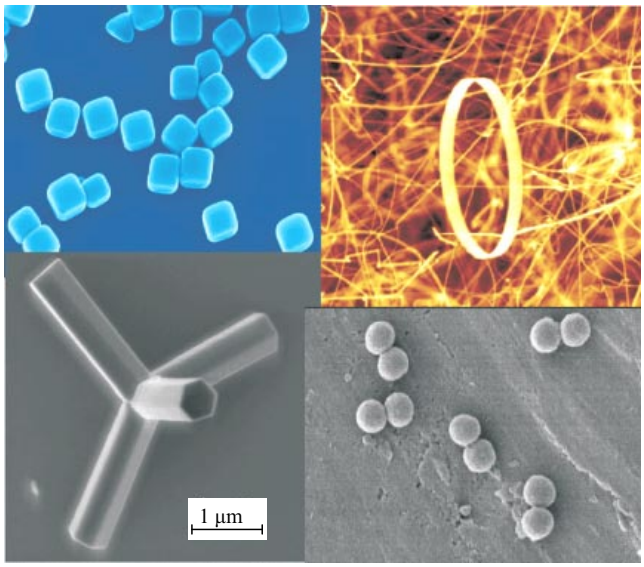

Figure 1. Examples of nanoparticles amenable to efficient synthesis techniques.

to be tuned so as to effectively interact with light or with elementary quantum systems like molecules and quantum dots.

These most important properties of plasmon nanoparticles have already allowed a range of new effects to be detected. First and foremost, the huge local fields that arise near nanoparticles lead to an increase of 10 – 14 orders of magnitude in the Raman scattering cross section, conceivably making individual molecule detection possible [2, 3]. The presence of local fields can be exploited to design marker-free techniques for determining the structure of DNA [4]. Using the complex spectral structure of plasmon nanoparticles, it proves possible to simultaneously enhance their light absorption and light emission properties, giving rise to high-performance fluorophores and nano-sized light sources [5]. Also, there are suggestions to use plasmon nanoparticles in the SPASER (Surface Plasmon Amplification by Stimulated Emission of Radiation) context [6]. Other than the above novel applications — ones that rely on plasmon nanoparticle physics — achievements in the field of nanoplasmonics can be used to improve the performance-to-cost ratio of, for example, solar batteries and LEDs. Furthermore, the small size of metal nanostructures combined with optically fast

processes occurring in them gives nanoplasmonics good promise for developing a new component base for computers and data processing devices [7].

Exactly how a localized plasmon should be defined is as yet an unsettled question, but a widely held view is that this is simply a resonance peak in the nanoparticle's light-scattering or light-absorption cross sections. This is often misleading though, because far from all localized plasmons can be readily detected or described as such ('dark' plasmons with zero dipole polarizability being an example). In our view, the term 'a localized plasmon' should be applied to the solutions of the problem covering free quasistatic oscillations in nanoparticles (the term 'free' meaning the absence of exciting fields), which reduces to the following Laplace equation boundary value problem:

$$\Delta\varphi_n^{\rm in}=0\,,\quad \Delta\varphi_n^{\rm out}=0\,,\quad \varepsilon_n\left.\frac{\partial\varphi_n^{\rm in}}{\partial\mathbf{n}}\right|_S=\left.\frac{\partial\varphi_n^{\rm out}}{\partial\mathbf{n}}\right|_S, \tag{1}$$

where $\varphi_n^{\rm in}$ and $\varphi_n^{\rm out}$ are the electric potentials of the plasmon eigenfunctions inside and outside of the particle, respectively, and $\partial\varphi_n/\partial\mathbf{n}|_S$ denotes the normal derivative at the boundary of the particle. The last of equations (1) ensures the fulfilment of a continuity condition of normal induction components. The mathematical complexity of the seemingly simple system (1) is enormous, as is the range of physical problems it encompasses.

It is the eigenfunctions $\mathbf{e}_n=-\nabla\varphi_n$ and eigenvalues ε_n of the permittivity that determine a localized plasmon oscillation. For finite-sized nanoparticles, the eigenvalues ε_n assume only negative (with zero imaginary part) discrete values, making localized plasmons very similar in this respect to ordinary atoms and molecules. What is extremely important here is that *the eigenvalues ε_n are of no relevance to the permittivity of the real material the nanoparticles are made of*.

Numerical studies of localized plasmons are conveniently carried out by using Eqn (1) in its integral form:

$$\sigma(\mathbf{r})=\frac{1}{2\pi}\,\frac{\varepsilon-1}{\varepsilon+1}\int_S \mathrm{d}^2\mathbf{r}'\sigma(\mathbf{r}')\,\frac{\mathbf{n}(\mathbf{r})(\mathbf{r}-\mathbf{r}')}{|\mathbf{r}-\mathbf{r}'|^3}\,,\quad \mathbf{r},\mathbf{r}'\in S, \tag{2}$$

where $\sigma(\mathbf{r})$ is the surface charge, $\mathbf{n}(\mathbf{r})$ is the outer normal to the particle's surface, and the integration is taken over the surface of the particle.

Once the solution of quasistatic problem (1) or (2) has been found, the solution of the actual problem with given exciting fields $\mathbf{E}^0(\mathbf{r})$ can be expressed in terms of the eigenfunctions and eigenvalues of the permittivity of localized plasmons as follows:

$$\mathbf{E}(\mathbf{r},\omega)=\mathbf{E}^0(\mathbf{r},\omega)+\sum_n \mathbf{e}_n(\mathbf{r})\,\frac{\left[\varepsilon(\omega)-1\right]}{\left[\varepsilon_n-\varepsilon(\omega)\right]}\,\frac{\int_V \mathbf{e}_n\mathbf{E}^0\,\mathrm{d}V}{\int_V \mathbf{e}_n^2\,\mathrm{d}V}\,, \tag{3}$$

where the integration is taken over the volume V of the particle, and $\varepsilon(\omega)$ is the frequency-dependent permittivity of the actual material of the nanoparticle. At those frequencies ω_n for which some of the denominators is close to zero, $\varepsilon_n\approx\varepsilon(\omega_n)$, a plasmon resonance occurs, which can, in principle, be observed. In the case of the Drude dispersion, the resonance plasmon frequencies can be found from the relationship

$$\omega_n=\frac{\omega_{\rm p}}{\sqrt{1-\varepsilon_n}}\,, \tag{4}$$

where $\omega_{\rm p}$ is the plasmon frequency of the metal. From Eqn (3), in turn, the polarizabilities, scattering and absorption cross sections, spontaneous emission rates of the atoms, etc. can be found.

The most important feature of quasistatic description (1) is that it narrows the problem to plasmon oscillations alone. Other particle's modes (whispering gallery modes) do not arise in this picture and so do not hamper obtaining and interpreting the results.

In fact, the above theory applies only to nanoparticles, i.e., when retardation effects are negligible. If the nanoparticles are considered to be finite in comparison with the wavelength, the eigenvalues ε_n acquire negative imaginary parts which are related to the emission of the plasmons and are given by

$$\Delta\varepsilon_m=-\mathrm{i}k^3\,\frac{(\varepsilon_m-1)^2}{6\pi}\,\frac{\left(\int_V \mathbf{e}_m\,\mathrm{d}V\right)^2}{\int_V \mathbf{e}_m^2\,\mathrm{d}V}\,. \tag{5}$$

In the simplest case of spherical nanoparticles of radius R_0, the problem for the eigenfunctions and eigenvalues of the permittivity has the solution

$$\varepsilon_n=-\frac{n+1}{n}-\Delta_n(ka)^2-2\mathrm{i}(ka)^3\delta_{n1}+\ldots\,,\quad n=1,2,3,\ldots\,, \tag{6}$$

$$\Delta_1=-\frac{12}{5}\,,\quad \Delta_2=-\frac{5}{14}\,,\quad \Delta_3=-\frac{56}{405}\,,\quad \ldots\,,$$

$$\varphi_{\rm in}=\left(\frac{r}{R_0}\right)^n Y_n^m(\theta,\varphi)\,,\quad \varphi_{\rm out}=\left(\frac{R_0}{r}\right)^{n+1} Y_n^m(\theta,\varphi)\,, \tag{7}$$

where r is the radius, and Y denotes spherical harmonics. The most important electron oscillation mode is the dipole mode, with $n=1$, and $\varepsilon_1=-2$.

For more composite and less symmetric nanoparticles, the resonance plasmon frequencies and the potentials of plasmon atoms have a more intricate form. For example, in the case of a metal nanoparticle in the form of a three-axis ellipsoid with half-axes $a_1>a_2>a_3$, the plasmon frequencies will be given by [8]

$$\varepsilon_{nm}(a_1,a_2,a_3)=\frac{E_n^m(a_1)\,F_n'^m(a_1)}{E_n'^m(a_1)\,F_n^m(a_1)}\,,\quad n=1,2,3,\ldots\,,\ m=1,2,\ldots,2n+1\,, \tag{8}$$

where E_n^m and F_n^m are the internal and external Lamé functions, and the prime denotes the derivative of a function with respect to its argument.

The nanoparticles of most practical importance are those having the shape of a cube — or rather being close to this shape, because the edges and tips of such nanoparticles are rounded off in the growth process [9] (see Fig. 1). Localized plasmons in this kind of nanoparticles are conveniently discussed by representing their surface parametrically in the form

$$x^n+y^n+z^n=a^n\,. \tag{9}$$

Here, $n=2$ and $n=\infty$ correspond to a sphere and a cube, respectively.

The dependences of the resonance values of the permittivity on the parameter n are depicted in Fig. 2. It is seen how the permittivity eigenvalues split and gradually transform into

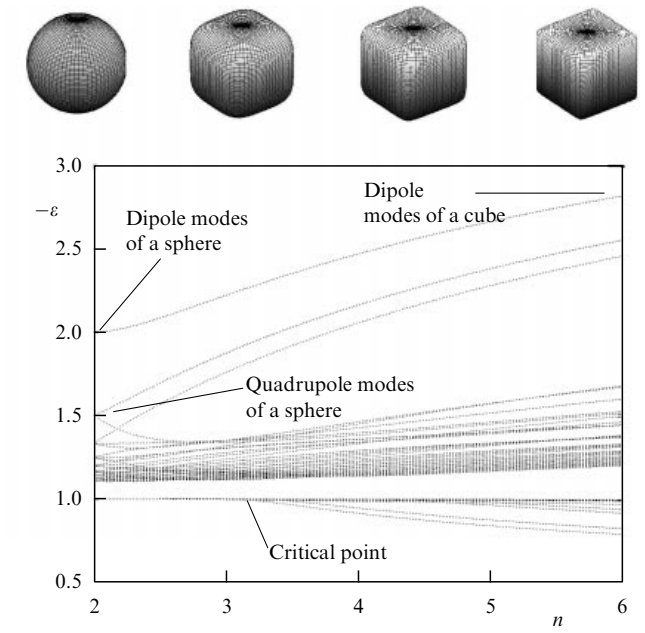

Figure 2. Spectrum of plasmon oscillations as a function of the shape of nanoparticles with cubic morphology.

those of a cube as the symmetry alters. Remarkably, at $n=2.5$ the plasmon spectrum branches with $\varepsilon > -1$ form, which are characteristic of a cube but not of a sphere. In fact, the plasmon spectra experience a phase transition at $n = 2.5$. A similar transition often occurs in other complex-shaped nanoparticles, as well. The spectra obtained are very important in providing pure spectroscopic means with which the shape-changing processes of nanoparticle crystallization or melting can be controlled.

Plasmon oscillations in a cluster comprising two spherical nanoparticles provide another impressive example of localized plasmons [10–12].

The full spectrum of plasmon oscillations we obtained for this system is depicted in Fig. 3. The region $\omega < \omega_p/\sqrt{2}$ ($\varepsilon < -1$) exhibits only symmetric and antisymmetric hybrid states which exist for any interparticle distances and which in the limit of large distances between nanospheres change in a

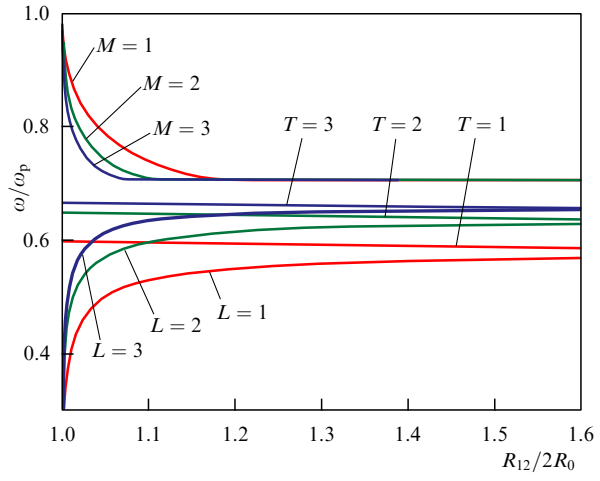

Figure 3. Plasmon oscillation spectrum for a two-nanosphere cluster versus the separation R_{12} ($m = 1$) between the spheres.

continuous manner to the corresponding states of weakly interacting localized plasmons with characteristics described by formulas (6), (7). It is these hybrid states which were studied in Refs [13–15].

In the region of $\omega_p \geqslant \omega > \omega_p/\sqrt{2}$ ($0 > \varepsilon > -1$), however, plasmon oscillations are only possible for small $[R_{12}/(2R_0) < 1.2]$ distances between the nanoparticles. At these distances, similar to nanoparticles of cubic morphology, the plasmon spectra of a two-nanoparticle cluster also show a phase transition.

In the region of small distances between nanospheres, the new branch of localized plasmon oscillations (M modes or plasmon molecules) has properties amenable to an analytical description [10–12]:

$$\varepsilon_m^M = -(M + m + \delta_m)\cosh\frac{R_{12}}{2R_0} + \ldots, \qquad (10)$$
$$M = 1, 2, 3, \ldots, \quad m = 0, 1, 2, \ldots,$$

where R_{12} is the center-to-center distance between the spheres, and

$$\delta_0 = \frac{1}{2}, \quad \delta_1 = -0.08578, \quad \delta_2 = -0.2639,$$
$$\delta_3 = -0.33, \ldots, \quad \delta_\infty = -\frac{1}{2}, \qquad (11)$$
$$\delta_m = -\frac{1}{2} - \frac{1}{2m} + \frac{1}{8m^3} - \frac{1}{16m^5} + \frac{5}{128m^7} - \ldots \quad (m > 0).$$

Large azimuthal numbers, $m \gg 1$, also allow simple asymptotic expressions to be obtained for the plasmon oscillation spectra of a two-sphere cluster, and the eigenfunctions of localized plasmons can also be expressed analytically in the small separation limit [10–12].

Figure 4 plots the spatial distribution in the xz plane of the wave function (potential) of localized plasmons.

In the axisymmetric ($m = 0$) case there is a qualitative correspondence between the spatial structure of the antisymmetric (L modes) and symmetric (T modes) plasmon oscillations and that of the wave functions of isolated spherical nanoparticles, namely, the positive charge resides on one semisphere, whereas a negative charge of the same amount (note the sphere electroneutrality requirement) locates at the opposite part of the sphere. In this case, interactions between plasmon atoms simply boil down to a certain redistribution of charge over opposite semispheres.

In the case of symmetric M modes appearing due to the phase transition, the situation is directly opposite and the charges concentrate in a small region close to the gap between the nanospheres. At those points on the spheres that are distant from the gap, the wave functions of plasmon molecules (M modes) become essentially zero.

As the distance between the nanospheres increases, the symmetric M modes become less localized — to eventually disappear at a critical distance, whereas the antisymmetric (L) and symmetric (T) modes remain unchanged as far as their localization is concerned.

The difference in localization between symmetric M modes, on the one hand, and the antisymmetric L modes and symmetric T modes, on the other, results in the former and the latter responding fundamentally differently to exciting fields. The L and T modes have a polarizability of the order of the nanosphere volume, $\alpha \sim R_0^3$, and interact effectively with uniform external fields of proper orientation

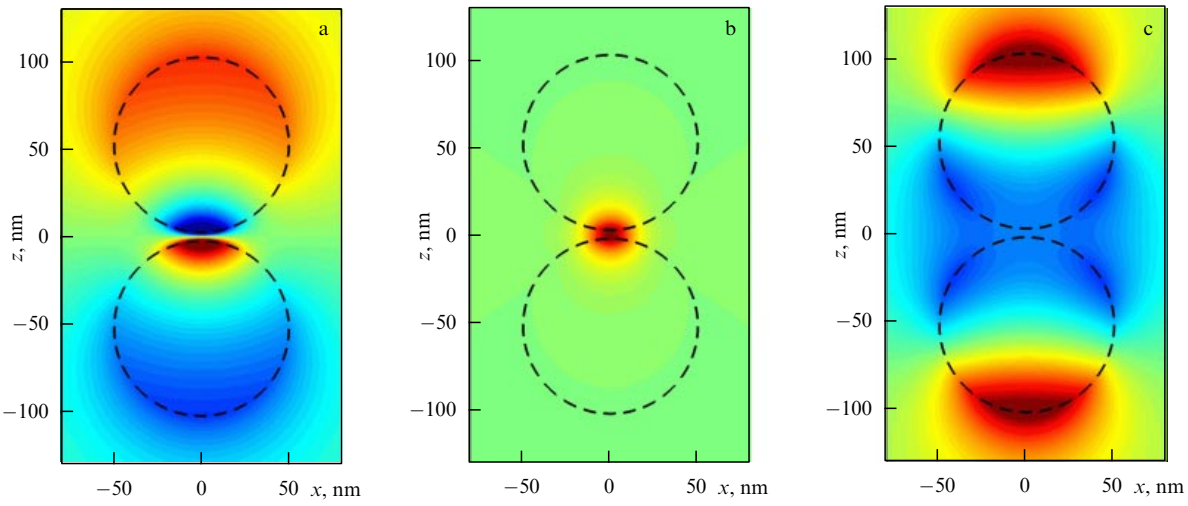

Figure 4. Spatial distribution of electric potential for (a) L modes, (b) M modes, and (c) T modes ($L, M, T = 1$) in the xz plane [$m = 0$, $R_{12}/(2R_0) = 1.05$].

and symmetry. M modes (plasmon molecules), in contrast, possess relatively low polarizability $\alpha \sim \Delta^3$, where Δ is the gap between the spheres, so their excitation by uniform optical fields is weak compared to the L and T modes. On the other hand, M modes interact effectively with strongly nonuniform fields that are localized near the sphere – sphere gap and arise due to the emission of atoms and molecules resided near the gap.

The discussion above was concerned with localized plasmons in a cluster comprising two identical nanospheres. The same localized plasmons also exist in clusters of two different nanospheres or two different bubbles in metal. For example, the spectrum of plasmon oscillations for two different spheres a small distance apart can be described by the expression

$$\frac{\varepsilon_1(\omega)-\varepsilon_3}{\varepsilon_1(\omega)+\varepsilon_3}\,\frac{\varepsilon_2(\omega)-\varepsilon_3}{\varepsilon_2(\omega)+\varepsilon_3} \approx \exp\left[(2N+2m-1)(\eta_2-\eta_1)\right], \tag{12}$$

$$N = 1, 2, 3, \ldots, \quad m = 0, 1, 2, \ldots,$$

where the parameter $\eta_2 - \eta_1$ can be found from the relationship

$$\cosh(\eta_2-\eta_1) = \frac{R_{12}^2 - R_1^2 - R_2^2}{2R_1R_2}, \tag{13}$$

and ε_1, ε_2, ε_3 are the permittivities of the first sphere, the second sphere, and the region in-between, respectively.

The strong localization of M modes suggests that what mainly determines their properties is the radii of curvature of the two almost touching surfaces and the distance between their centers. Therefore, for any smooth nonspherical particles the properties of M modes that form in the gap between them can be estimated by considering M modes in two spheres approximating the nonspherical particles at their point of contact.

Two closely spaced semi-infinite bodies give rise to a more complex situation because in this case some of the charges can move arbitrarily far from the region of contact and the spectrum becomes continuous — with the result that localized plasmons do not, strictly speaking, exist in such systems. However, stable plasmon oscillations similar to antisymmetric L modes and symmetric M modes exist in this case, as well [12].

As already noted, the unique properties of localized plasmons — nanolocalization, optical frequencies, shape-tuned resonances — are of interest for many applications.

Also, the strong localization of M modes appears to show promise for a range of applications, especially those relying on the effective interaction of nanolocalized light sources (molecules and nanocrystalline quantum dots) with nanoparticles and nanostructures, and for nanoelectromechanical devices [16] where van der Waals forces are of importance.

As is known, van der Waals forces relate to the spatial dependence of vacuum-fluctuation energy density. In the case of closely spaced plasmon nanoparticles, the van der Waals energy is dominated by contributions from the zero-point oscillations of localized plasmons.

For two identical plasmon nanospheres, the van der Waals energy consists of contributions from the zero-point oscillations of antisymmetric L modes and symmetric T and M modes:

$$U_{\mathrm{vdW}} = \frac{\hbar}{2}\left(\sum_{M=1}^{\infty}\omega_{M0} + \sum_{L=1}^{\infty}\omega_{L0} + \sum_{T=1}^{\infty}\omega_{T0}\right) + \hbar\left(\sum_{M,m=1}^{\infty}\omega_{Mm} + \sum_{L,m=1}^{\infty}\omega_{Lm} + \sum_{T,m=1}^{\infty}\omega_{Tm}\right). \tag{14}$$

Although the contributions from different modes are given by formally identical expressions, the physical consequences they produce are totally different. It is seen from Fig. 3 that the energies (frequencies) of antisymmetric states (L modes) increase with intersphere distance, leading to attraction between the particles. In contrast, the energy of M modes decreases with distance, making the nanospheres repel. Symmetric T modes also give rise to a very weak repulsion.

The plot in Fig. 5, obtained in Ref. [17] by directly summing all the modes in Eqn (14), shows the way in which contributions from various plasmonic states to the van der Waals energy vary with the separation between the spheres. As expected, the symmetric and longitudinal antisymmetric modes lead, respectively, to the repulsion and attraction of nanoparticles. It turned out unexpected that

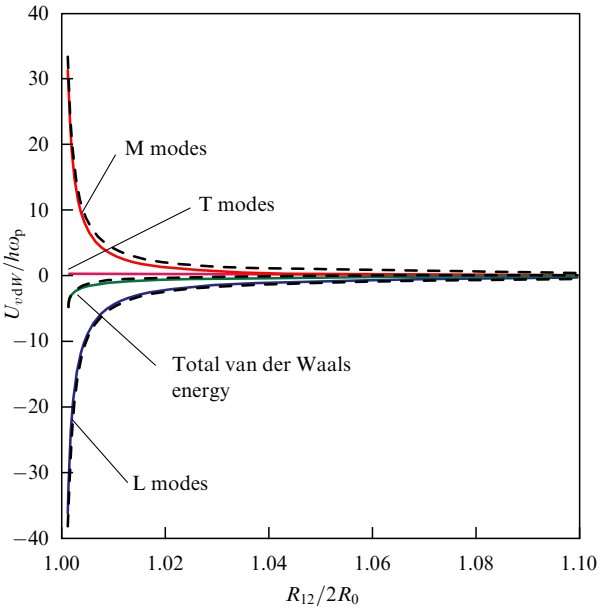

Figure 5. Van der Waals energy due to various plasmonic states as a function of separation between the spheres.

the repulsive contribution due to M modes is nearly equal to the attractive contribution caused by L modes. As a result, the total van der Waals energy increases with separation between the spheres — which reveals its attractive nature — but is an order of magnitude smaller than would be obtained by ignoring the M modes we discovered.

The direct measurement of van der Waals forces between plasmon nanoparticles provides a basis for experimentally verifying the existence of plasmon molecules (M modes).

The fact that M modes very effectively interact with strongly nonuniform fields suggests that optical interaction between molecules and M modes can be used in developing various single-molecule detectors or quantum dots. Figure 6 depicts the emission wavelength dependence of the radiative spontaneous decay rate of various kinds of molecules residing in the gap between two nanospheres. The nanospheres are taken to be made either of Na atoms with plasmon resonances in the optical region (Fig. 6a) or of SiC with phonon–polariton resonances in the infrared region (Fig. 6b). The peaks on the right-hand side of Fig. 6 correspond to the interaction of an ordinary molecule with T modes, whereas those on the left correspond to the interaction of localized plasmons with M modes.

Inspection of Fig. 6 shows that, similarly to the case of the van der Waals energy, the interaction with M modes is of more significance than that with symmetric T modes. It is also of extreme importance that a uniform external field is inefficient for exciting M modes (plasmon molecules), meaning that efficient single-molecule nanodetectors can be developed by using two-, or more, nanosphere clusters with geometry allowing excitation of plasmon molecules with a fixed frequency. These nanodetectors cannot practically be excited by external fields having the oscillation frequency of the M modes and will therefore have a high signal-to-noise ratio.

On the other hand, the effective interaction of plasmon molecules with ordinary atoms and molecules can be employed to develop SPASER and nanolaser type devices for operating singly or in a lattice.

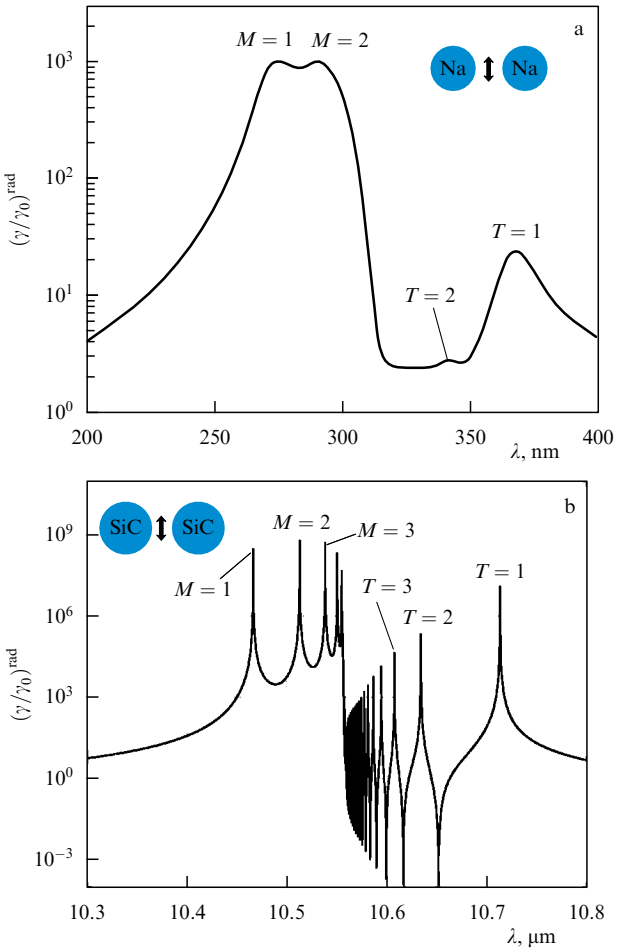

Figure 6. Relative radiative spontaneous decay rate of a molecule residing in the gap between two nanospheres as a function of the molecule's emission wavelength for (a) an Na nanosphere [18], and (b) an SiC nanosphere [19]. In either case, $R_{12}/(2R_0) = 1.5$. The dipole moment of the atom is directed as shown by the arrow.

To summarize, this report presents the general theory and the results of investigation of plasmon oscillations in separate nanoparticles and nanoparticle clusters. It was demonstrated that changing the shape of nanoparticles causes radical changes — specifically, plasmon phase transitions — in the spectra of localized plasmons. It was shown that the localized plasmons discussed in this report are an important concept for describing nanoelectromechanical systems and single-molecule nanodetectors, as well as for spectroscopically monitoring the shape of nanoparticles in the process of their synthesis.

Whereas this report was concerned with localized plasmons in nanoparticles of ordinary materials with $\varepsilon < 0$, much recent attention has been focused on metamaterials with both permittivity and permeability being negative [20]. Localized plasmons in nanoparticles produced from such materials have important differences from those discussed here [21] and can therefore naturally be called metaplasmons.

Acknowledgments. The author gratefully acknowledges the financial support provided by the Russian Foundation for Basic Research (grants Nos 05-02-19647, 07-02-01328) and the RAS Presidium.

References

1. Raether H *Surface Plasmons on Smooth and Rough Surfaces and on Gratings* (Berlin: Springer-Verlag, 1988)
2. Moskovits M et al., in *Optical Properties of Nanostructured Random Media* (Topics in Applied Physics, Vol. 82, Ed. V M Shalaev) (Berlin: Springer-Verlag, 2002) p. 215
3. Wang Z et al. *Proc. Natl. Acad. Sci. USA* **100** 8638 (2003)
4. Lakowicz J R et al. *J. Phys. D: Appl. Phys.* **36** R240 (2003)
5. Guzatov D V, Klimov V V *Chem. Phys. Lett.* **412** 341 (2005)
6. Bergman D J, Stockman M I *Phys. Rev. Lett.* **90** 027402 (2003)
7. Zia R et al. *Mater. Today* **9** (7–8) 20 (2006)
8. Klimov V V, Guzatov D V *"Opticheskie svoistva trekhosnogo nanoellipsoida i ikh vliyanie na izluchenie atomov i molekul"* ("Plasmon oscillations in ellipsoidal nanoparticles: beyond dipole approximation") (in preparation)
9. Sun Y, Xia Y *Science* **298** 2176 (2002)
10. Klimov V V, Guzatov D V *Phys. Rev. B* **75** 024303 (2007)
11. Klimov V V, Guzatov D V *Kvantovaya Elektron.* **37** 209 (2007) [*Quantum Electron.* **37** 209 (2007)]
12. Klimov V V, Guzatov D V *Appl. Phys. A* **89** 305 (2007)
13. Claro F *Phys. Rev. B* **25** 7875 (1982)
14. Ruppin R *Phys. Rev. B* **26** 3440 (1982)
15. Nordlander P et al. *Nano Lett.* **4** 899 (2004)
16. Ekinci K L, Roukes M L *Rev. Sci. Instrum.* **76** 061101 (2005)
17. Klimov V V, Lambrecht A, arXiv:0712.4067
18. Palik E D (Ed.) *Handbook of Optical Constants of Solids* (Orlando: Academic Press, 1985)
19. Engelbrecht F, Helbig R *Phys. Rev. B* **48** 15698 (1993)
20. Soukoulis C M, Linden S, Wegener M *Science* **315** 47 (2007)
21. Klimov V V *Opt. Commun.* **211** 183 (2002)

PACS numbers: 52.27.Ep, 97.10.Ld, 97.60.Jd
DOI: 10.1070/PU2008v051n08ABEH006596

Electron – positron plasma generation in the magnetospheres of neutron stars

Ya N Istomin

1. Introduction

In this report we discuss the processes of the generation of relativistic electron – positron plasma in magnetospheres of rotating magnetized neutron stars. Both not very strong magnetic fields, $B \simeq 10^{12}$ G, typical for radio pulsars, and superstrong magnetic fields, $B \simeq 10^{14} - 10^{15}$ G, typical for so-called magnetars, are considered. It is shown that superstrong magnetic fields do not suppress particle production. Intervals of neutron star parameters, first of all rotation periods and magnetic field strengths, allowing effective plasma generation have been found.

Neutron stars are the smallest observed stars in the Galaxy. Their radius R is around 10 km (for comparison, the solar radius amounts to 7×10^5 km). So, the ratio of the radius of a neutron star to that of ordinary stars is about 10^{-5}. However, with such a small radius, neutron stars have a mass M on the order of the solar one $M_\odot$, with the average magnitude being $1.4M_\odot$. The mean density of the neutron star matter is $\bar{\rho} = 3M/4\pi R^3 = 7 \times 10^{14}$ g cm^{-3}, which exceeds the standard nuclear density $\rho_0 = 2.8 \times 10^{14}$ g cm^{-3} by several times ($\bar{\rho} \simeq 2.5\rho_0$). Therefore, a neutron star can be considered as a huge atomic nucleus with a radius of about 10 km. The matter density at the center of the star can exceed the nuclear one by 10–20 times. At such densities in the neutron star center, pion, hyperon, and kaon condensations are made possible. The possibility of the appearance of quarks, mostly strange, is also discussed. Such stars are termed strange stars.

The body of a neutron star consists of outer and inner crusts, where the neutronization of matter occurs, and of outer and inner cores. The number of protons and electrons in the inner crust and outer core is much smaller than the number of neutrons, the ratio being of the order of several percent. Neutrons and protons probably form superfluid and superconducting pairs, so that neutron star matter possesses superfluid and superconductive properties. It should also be noted that the gravitational energy of a neutron star amounts to a substantial fraction of its rest energy: $E_g = GM^2/R \simeq 5 \times 10^{53}$ erg $= 0.2Mc^2$, where G is the Newtonian constant of gravitation.

The existence of neutron stars was predicted by Baade and Zwicky [1] in 1934, two years after the discovery of neutrons. Despite their small size, neutron stars are among the most active stars, radiating energy in the entire electromagnetic spectral range from radio waves to ultra-high energy photons beyond 1 TeV.

Neutron stars were discovered in 1967 by Bell and Hewish [2] as sources of periodic radio emission — radio pulsars. In 1974, Hewish was awarded the Nobel Prize in Physics for his decisive role in the discovery of pulsars.

Presently, more than 1500 radio pulsars are known. Their pulse-repetition intervals, i.e., the periodicity of recurring radio pulses, are very stable and span the range from 1.5 ms to 8.5 s. The high stability and small intervals can only be explained by the rotation of a small body with radius $R < 5 \times 10^7$ cm. Only neutron stars have such small radii. A constant increase in the pulse-repetition intervals P of radio pulsars with time is also observed, $\mathrm{d}P/\mathrm{d}t \simeq 10^{-15}$ s s^{-1}, implying a loss in the rotational energy of a neutron star. The measured energy loss $\mathrm{d}E/\mathrm{d}t = (2\pi)^2 IP^{-3}\,\mathrm{d}P/\mathrm{d}t$ for the standard moment of inertia $I = 10^{45}$ g cm^2 of a neutron star is on the order of $\mathrm{d}E/\mathrm{d}t \simeq 4 \times 10^{31}$ erg s^{-1}. However, rapidly rotating neutron stars actually lose much higher energy. For example, the Crab Nebula pulsar emits 10^{38} erg s^{-1}, which is by many orders higher than the solar luminosity. The energy emitted in the radio frequency band amounts to only a tiny fraction, $10^{-5} - 10^{-6}$, of the total energy losses. The most powerful radio pulsars also radiate in other spectral ranges, including the optical, X-ray, and gamma-ray ranges. The emission power increases with frequency, but nevertheless remains much smaller than the total energy losses. The question arises as to what is mainly emitted by a rotating neutron star?

In addition to being radio pulsars, neutron stars are also the sources of

(a) powerful X-ray emission, both periodic (X-ray pulsars) and irregular. These are neutron stars in close binary stellar systems in which the star-companion provides the neutron star with matter accreting onto it. The energy liberated during accretion amounts to $\simeq 0.2$ of the rest energy of the infalling flux of matter;

(b) gamma- and X-ray bursts. These are anomalous X-ray pulsars (AXPs) and soft gamma repeaters (SGRs). Both these groups are combined into one class of the so-called magnetars. They comprise neutron stars with ultrahigh surface magnetic fields of $10^{14} - 10^{15}$ G;

(c) steady X-ray emission from central compact objects (CCOs) in supernova remnants. These are neutron stars formed during the core collapse of pre-supernova stars;